

# Fabrication of silicon membrane using fusion bonding and two-step electrochemical etch-stopping

B. K. JU, M. H. OH

*Division of Electronics and Information Technology, Korea Institute of Science and Technology 39-1, Haweolgog-dong, Seongbuk-gu, Seoul 136-791, Korea*

K. H. TCHAH

*Department of Electronics Engineering, Korea University Anam-dong, Seonbuk-gu, Seoul 136-701, Korea*

A new type of silicon membrane structure was fabricated using wafer fusion bonding and two-step electrochemical etch-stopping methods. An "active wafer" of p-type epi/n-type epi/p-type substrate was first electrochemically etched to form a shallow cavity on the p-type epitaxial layer. Then, the cavity-formed side was fusionally bonded with p-type silicon "working wafer" and, afterwards, the p-type substrate of the active wafer part was removed by a second electrochemical etch-stopping leaving only the n-type membrane on the shallow cavity. Using the new membrane structure in mechanical sensors, more precise control of cavity depth and membrane thickness was achievable and the influence of crystalline imperfections on the sensing circuits located near the bonding seam was avoidable.

## 1. Introduction

In addition to the silicon-on-insulator (SOI) field, a silicon fusion bonding (SFB) method has widely been employed in integrated sensor fabrication, such as silicon pressure, or acceleration sensors [1–3]. The pressure sensor was made using a thin silicon membrane, as shown in Fig. 1a, which was typically formed by a deep anisotropic etching from the rear side. This sensor benefitted greatly from the availability of the SFB process, as in Fig. 1b, particularly in chip size, over-pressure protection, and batch processing sequence [3].

If, however, mechanical imperfections existed at the bonding interface between the bonded wafer pair due to incomplete wafer–wafer contact or misalignment, some cracks and dislocation loops were easy to generate around the sites. As the bonding and after-thinning steps proceeded, the imperfections grow gradually and might propagate to the top surface on which some sensing resistors would be located. This might become a serious problem for the piezoresistive-type sensor where sensing resistors often lie near the membrane edge.

In these experiments, we devised a new membrane structure, shown in Fig. 1c, in order to alleviate these problems, and also a processing technique by which its mechanical dimensions could be more precisely controlled.

## 2. Shallow cavity formation using the first electrochemical etch-stopping

A 4 in. (100)-oriented silicon wafer was used, on which

n- and p-type epitaxial layers had been grown alternatively (Fig. 2), as an "active wafer". The thickness of the n- and p-type epilayers corresponded to the cavity depth and membrane thickness to be formed, respectively. The wafer was oxidized to form a 0.05  $\mu\text{m}$  thick  $\text{SiO}_2$  film as an etch mask and a square-shaped oxide window,  $1.0 \times 1.0 \text{ mm}^2$ , was photographically opened on the p-type epilayer. Then the oxide film on the rear side was stripped off and 0.2  $\mu\text{m}$  thick silicon doped aluminium electrode was deposited to provide ohmic contact.

The prepared sample was electrochemically etched in the etching bath depicted in Fig. 3, and catalysed EPW solution was employed as an "F etchant" in accordance with the literature [4, 5]. The composition was ethylenediamine (E, 4275 ml), pyrocatechol (P, 1368 gr), water (W, 1368 ml) and pyrazine (25.65 gr). The etching temperature was fixed at  $115 \pm 0.5^\circ\text{C}$ . A magnetic stirrer and a reflux condenser were installed in this apparatus and  $250 \text{ cm}^3 \text{ min}^{-1}$   $\text{N}_2$  bubbling was conducted around the bottom. A +1.8 V bias was also applied to the wafer through the aluminium electrode from a constant voltage source as an etch-stopping potential, and the solution was grounded by a platinum mesh.

Fig. 4 shows the current curve in solution during silicon etching. This type of curve has been observed for the electrochemical etching in solutions of  $\text{KOH-H}_2\text{O}$  or  $\text{N}_2\text{H}_4\text{-H}_2\text{O}$  etc. [6–9]. After dipping the sample, no current flowed in solution during the initial stage of 2–3 min indicating the presence of a thin native oxide [10]. In 5 min, hydrogen bubbles started to be generated from the unpassivated surface

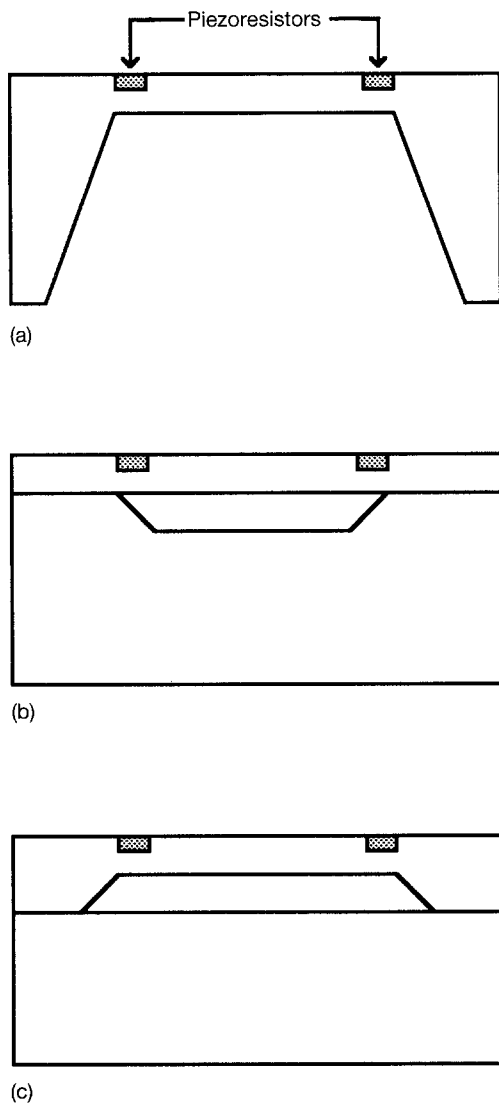


Figure 1 Silicon pressure sensor chips having thin membranes made by (a) deep anisotropic etching, (b) typical bonding and thinning, and (c) the new method devised in this work.

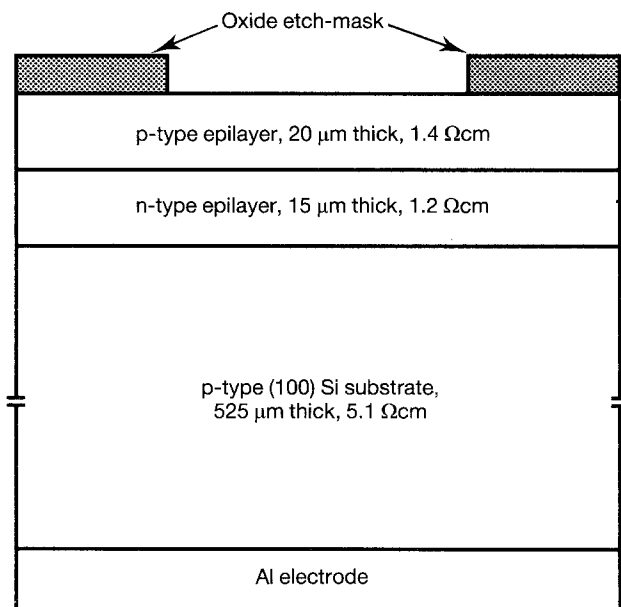


Figure 2 Specification of the "active wafer" to be electrochemically etched, for the first time.

of the p-type epilayer and the current level reached approximately  $0.2 \text{ mA cm}^{-2}$ . This current was considered to be the reverse current through the p-n

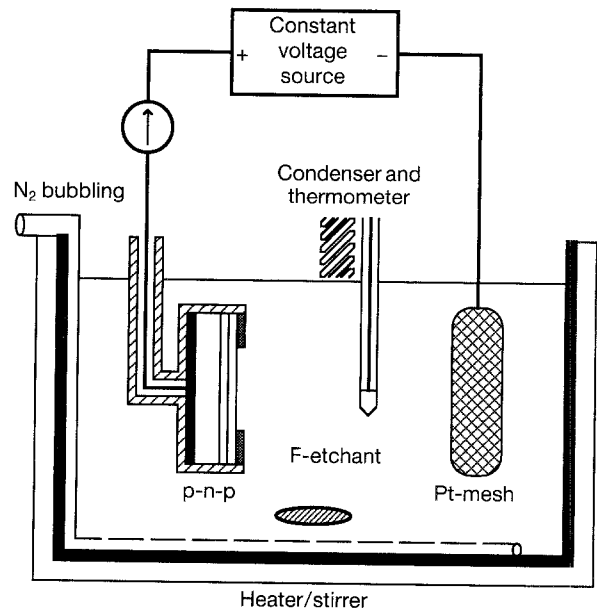


Figure 3 The electrochemical etching system.

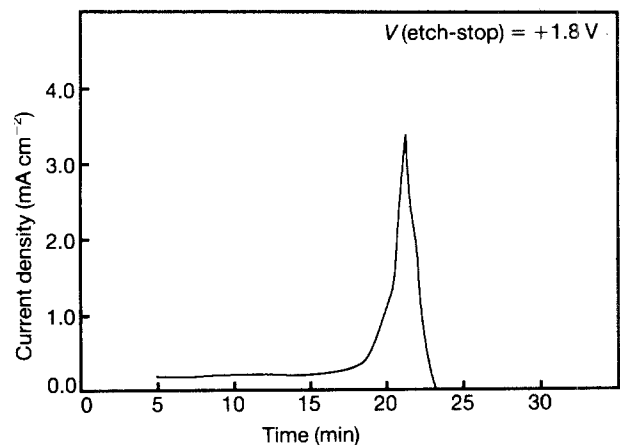


Figure 4 Measured current curve during the first electrochemical etching.

junction between n-type epilayer and p-type epilayer as shown in Fig. 2, while most of the electrical voltage drops occur in the depletion region. After 20 min, the current increased abruptly to a peak value of  $3.3 \text{ mA cm}^{-2}$ , indicating that the unpassivated p-type epilayer was completely removed and etch-stopping occurred on the surface of the n-type epilayer. At that point, an anodic oxide began to be formed on the etched surface due to the large current flowing through the "Al electrode/p-type sub./n-type epi/ionized solution/Pt cathode" path, and it acted as an etch mask [6]. After that, the current value was reduced to almost zero within 1 min and hydrogen bubbling was diminished.

In order to investigate the etch-stopping behaviour, the cavity-formed wafer was angle-lapped with a bevel angle of  $2^{\circ}52'$  and the n-type epilayer stained by dipping it into  $(\text{CuSO}_4 + 5\text{H}_2\text{O})0.8 \text{ gr} : \text{HF}1 \text{ ml} : \text{H}_2\text{O} 100 \text{ ml}$  solution under an intense light source. It was noticed that etch-stopping occurred exactly on the n-type epilayer, as shown in Fig. 5. The thickness and refractive index of the anodic oxide formed on the

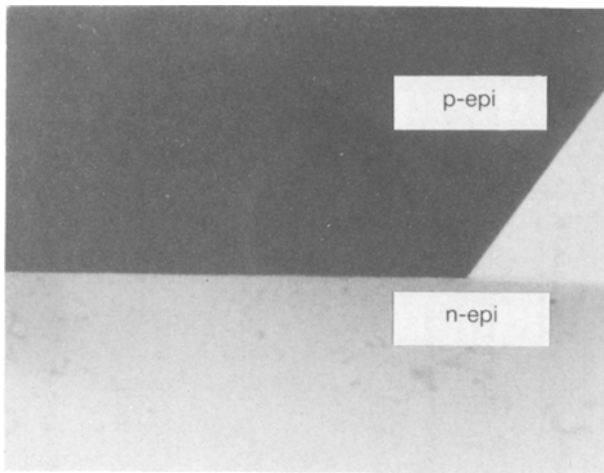


Figure 5 The shallow cavity stained after etch-stopping.

n-type epilayer were measured to be  $0.0085 \mu\text{m}$  and  $1.48$ , respectively, by an ellipsometer.

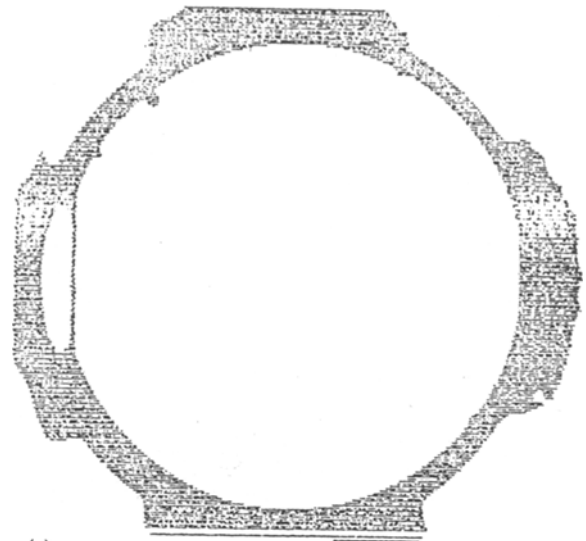
### 3. Fusion bonding between “active” and “working” wafers

After removal of the oxide and aluminium films of the prepared “active wafer”, on which a  $1 \times 1 \text{ mm}^2$  sized and  $20 \mu\text{m}$  deep cavity had been formed, the wafer was fusion-bonded with a p-type “working wafer”. The “working wafer” had the same specification as that of the p-type substrate in the “active wafer”. Prior to bonding, the two wafers were cleaned according to the standard RCA method [11] and dipped into 6 parts  $\text{H}_2\text{O}$ :1 part  $\text{H}_2\text{O}_2$ :4 parts  $\text{NH}_4\text{OH}$  solutions at  $57^\circ\text{C}$  for 2 min in order to form a hydrophilic layer on the surface to be bonded. Then the wafers were rinsed in deionized water and spin-dried. They were stabilized for 30 s at room temperature in nitrogen ambient and Van der Waals-bonded after contacting each other. Immediately afterwards, the weakly bonded wafer pair was annealed at  $1100^\circ\text{C}$  for 90 min in nitrogen. The above process made a complete bonding between two wafers without any voids and the bonding strength reached about  $165 \text{ kg cm}^{-2}$ [12].

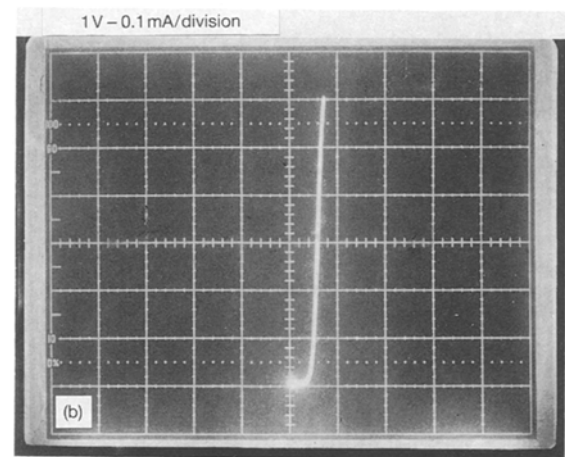
Fig. 6a and b show the ultrasonic image for a bare p-type Si/n-type Si wafer pair-bonded according to the above-mentioned sequences and the forward current-voltage characteristic for the bonded diode of  $2 \times 2 \text{ mm}^2$  size which was selected from the wafer pair [12]. Based on these experiments, we could infer that the bonded “active-working wafer” pair might have good mechanical and electrical continuity at the bonding interface. Fig. 7 shows the shallow cavity and bonding interface in the sample processed up to the above step. There was no transient region observable between wafer and wafer interface, even at  $\times 50\,000$  SEM.

### 4. Membrane formation using the second electrochemical etch-stopping

The bonded wafer pair was prepared as shown in Fig. 8a for carrying out a second electrochemical etch-



(a)



(b)

Figure 6 (a) Ultrasonic image and (b) the diode property of the p-type/n-type silicon wafer pair stabilized and annealed at  $1100^\circ\text{C}$  for 90 min in a nitrogen ambient.

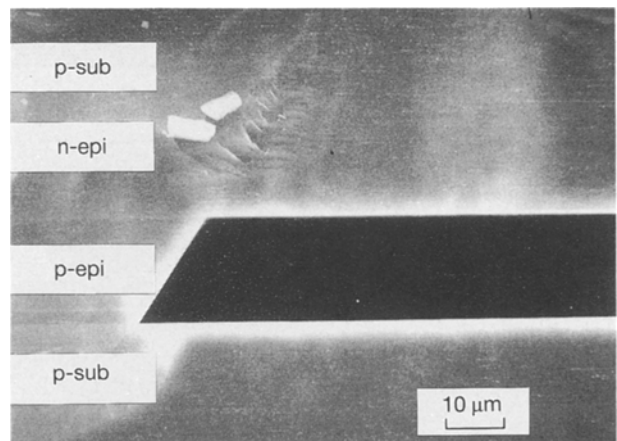


Figure 7 Sample cross-section after fusion bonding.

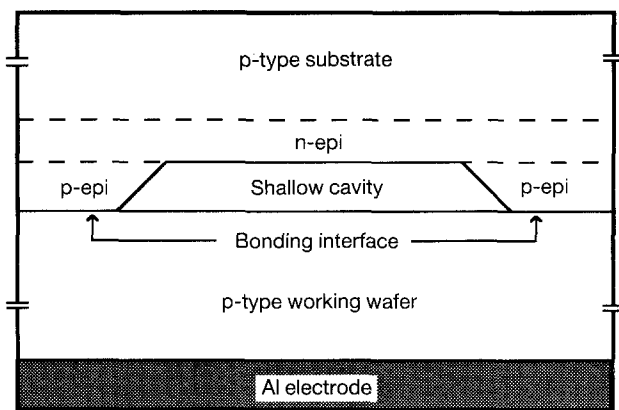
stopping. An aluminium electrode was evaporated on to the rear side of the “working wafer”. The prepared sample was electrochemically etched in the apparatus described in Section 2, except that a higher etch-stopping potential,  $+3.2 \text{ V}$ , was applied to the electrode. The value was properly selected by considering possible potential drops which might occur near the

bonding interface or in the thick bulk region of the “working wafer”.

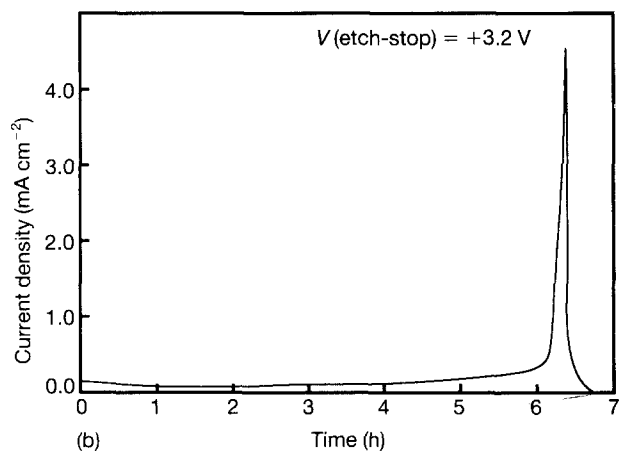
The current curve observed during etching, as shown in Fig. 8b, had a very similar shape to that in the first etching process. The current path was connected through “Al electrode/p-type substrate/p-type epilayer/n-type epilayer/p-type substrate/solution/Pt cathode”, and therefore, a potential barrier existed at the n-type epi/p-type substrate interface in the “active wafer”. The etch-stopping occurred at the site after the p-type substrate was completely etched out.

The current peak observed after 385 min etching was acceptable considering that the average etch rate of the (100)-oriented silicon was about  $81 \mu\text{m min}^{-1}$  under the solution used [4]. Because of a higher applied potential, the peak value of  $4.5 \text{ mA cm}^{-2}$  showed a  $1.2 \text{ mA cm}^{-2}$  increase over the value of  $3.3 \text{ mA cm}^{-2}$  for the first etching. In addition the anodic oxide formed on the fabricated n-type membrane had a thickness of  $0.0099 \mu\text{m}$  and a refractive index of 1.45.

Fig. 9a and b show cross-sections of the fabricated n-type silicon membrane near the right and left corners, respectively. Its thickness was measured to be about  $15.9 \mu\text{m}$  which increased about  $0.9 \mu\text{m}$  over the expected value. We could infer that the result was due to a carrier redistribution which might happen at the n-type epi/p-type substrate interface during the high-temperature fusion bonding process.



(a)



(b)

Figure 8 (a) Sample illustration of the second electrochemical etching and (b) the current curve observed during etching.

We also discovered some white residue [5] and the orange peel phenomenon [13] on the membrane surface after anodic oxide stripping in buffered HF. In order to eliminate the undesired material and to control the membrane thickness more precisely, a final Syton polishing step [13] was added on the membrane surface, and a  $\sim 1 \mu\text{m}$  thick layer was removed. Fig. 10 shows the surface roughness of the polished membrane which indicated a homogeneity of  $15 \pm 0.1 \mu\text{m}$  in thickness.

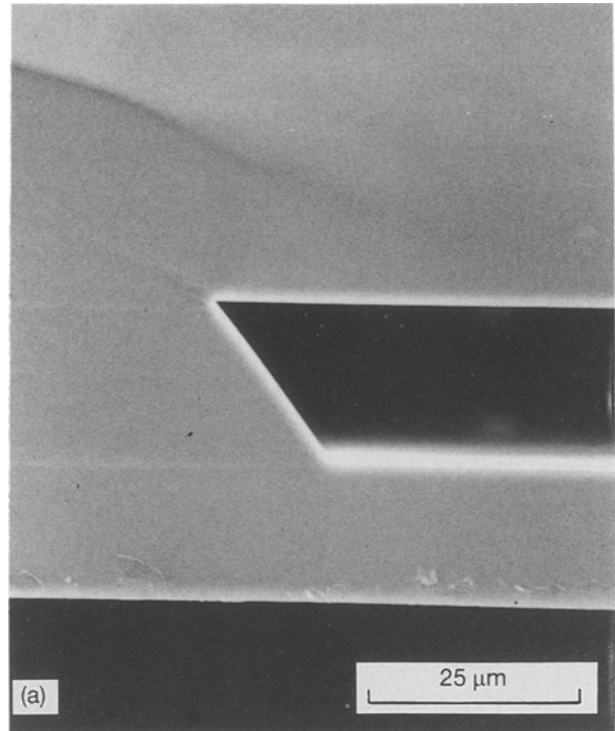


Figure 9 Scanning electron micrographs of (a) the right and (b) the left side of the fabricated silicon membrane.

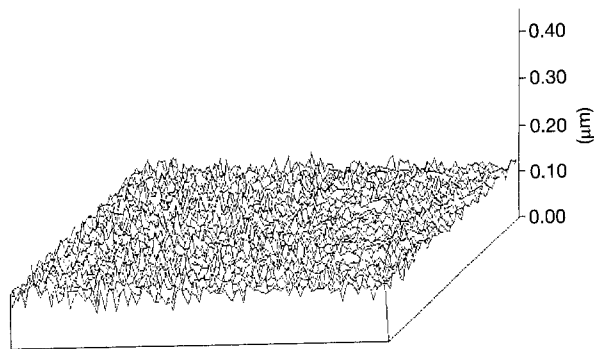


Figure 10 Surface roughness of the silicon membrane after a final Syton polishing. Measured area  $800\ \mu\text{m} \times 50\ \mu\text{m}$ .

## 5. Conclusion

New technique for making a silicon membrane by self etch-stopping and fusion bonding processes has been investigated. Attempts are now underway to make a multiple number of thin membranes on a 4 in. full wafer using the technique, which may be very useful in batch-fabrication of silicon pressure sensors etc. The methods can also be applied to the formation of other micro-mechanical structures, such as beams, plates, etc.

## References

1. L. CHRISTEL, K. PETERSEN, P. BARTH, F. POURAHMADI, J. MALLON Jr and J. BRYZEK, *Sensors Actuat. A21-A23* (1990) 84.
2. K. PETERSEN, J. BROWN, T. VERMEULEN, P. BARTH, J. MALLON Jr and J. BRYZEK, *ibid. A21-A23* (1990) 96.
3. P. W. BARTH, *ibid. A21-A23* (1990) 919.
4. A. REISMAN, M. BERKENBLIT, S. A. CHAN, F. B. KAUFMAN and D. C. GREEN, *J. Electrochem. Soc.* **126** (1979) 1406.
5. X.-P. WU, Q.-H. WU and W. H. KO, *Sensors Actuat.* **9** (1986) 333.
6. H. HIRATA, S. SUWAZONO and H. TANIGAWA, *J. Electrochem. Soc.* **134** (1987) 2037.
7. R. L. GEALER, H. K. KARSTEN and S. M. WARD *ibid.* **135** (1988) 1180.
8. B. KLOECK, S. D. COLLINS, N. F. DE ROOJI and R. L. SMITH, *IEEE Trans. Electron Devices* **36** (1989) 663.
9. Y. P. XU and R. S. HUANG, *J. Electrochem. Soc.* **137** (1990) 948.
10. M. MATSUOKA, Y. ARAI and Y. YOSHIDA, *Jpn J. Appl. Phys.* **27** (1988) 784.
12. B. K. JU, M. H. OH and K. H. TCHAH, *J. Mater. Sci.* **28** (1993) 1168.
13. J. HAISMA, G. A. C. M. SPIERINGS, U. K. P. BIERMANN and J. A. PALS, *Jpn. J. Appl. Phys.* **28** (1989) 1426.

Received 8 June 1992

and accepted 9 August 1993